Research Square

Preprints are preliminary reports that have not undergone peer review.
They should not be considered conclusive, used to inform clinical practice,
or referenced by the media as validated information.

A Pressed Pinus koraiensis Leaf Juice-Coconut Water Formulation Enhances Antioxidant Defense and Attenuates Inflammatory, Metabolic, and Intestinal Epithelial Stress In Vitro

Leeseon An
Kyung Hee University
Jaehee Hwang
Kyung Hee University
Hyo-Jeong Lee
strong79@khu.ac.kr

Kyung Hee University

Article

Keywords: Pinus koraiensis, pressed juice, coconut water, antioxidant activity, glutathione, functional food

Posted Date: November 11th, 2026

DOI: https://doi.org/10.21203/rs.3.rs-11440558/v1

License: This work is licensed under a Creative Commons Attribution 4.0 International License.
Read Full License

Additional Declarations: No competing interests reported.

A Pressed *Pinus koraiensis* Leaf Juice-Coconut Water Formulation Enhances Antioxidant Defense and Attenuates Inflammatory, Metabolic, and Intestinal Epithelial Stress In Vitro

Leeseon An [1†], Jaehee Hwang[1], and Hyo-Jeong Lee [1,2 *]

[1]Department of Science in Korean Medicine, Graduate School, College of Korean Medicine, Kyung Hee University, 26, Kyungheedae-ro, Dongdaemun, Seoul, 02447, Korea.

[2]Department of Cancer Preventive Material Development, Graduate School, College of Korean Medicine, Kyung Hee University, 26, Kyungheedae-ro, Dongdaemun, Seoul, 02447, Korea.

*Corresponding author (H.-J.L.) strong79@khu.ac.kr(0000-0003-1946-7842)

Contributing authors: iseony77@khu.ac.kr(0009-0001-6878-8282); hjh8267@khu.ac.kr(0009-0008-5755-3630)

Abstract

Pinus koraiensis leaves are a potential source of health-promoting phytochemicals. However, previous studies have primarily examined ethanol extracts or oil-based preparations. Here, we developed a food-compatible formulation consisting of pressed Korean pine leaf juice (PKJ) and coconut water (CW), designated PC, and evaluated its biological activities in vitro. PC exhibited greater antioxidant activity and higher phenolic and flavonoid assay responses than either component alone. Literature-based network analysis identified candidate targets associated with oxidative stress and inflammation, including BCL2, CASP3, HMOX1, IL6, NFE2L2, and NOS2. In LPS-stimulated THP-1 cells, PC suppressed iNOS/NO and pro-inflammatory cytokine responses. In HepG2 cells, PC restored glutathione-related antioxidant defense and Nrf2 expression under H_2O_2-induced oxidative stress and attenuated fructose-induced lipogenic and inflammatory responses. In H_2O_2-stimulated Caco-2 cells, PC restored glutathione-dependent antioxidant defense, suppressed iNOS/NO responses, and recovered GLP-1, ZO-1, and claudin-1 expression. Collectively, PC attenuated oxidative, inflammatory, metabolic, and intestinal epithelial stress, supporting its potential as a functional food formulation.

Keywords: *Pinus koraiensis*; pressed juice; coconut water; antioxidant activity; glutathione; functional

food.

1. Introduction

Pinus koraiensis, commonly known as Korean pine, is a coniferous species native to Northeast Asia, including Korea, China, Russia, and Japan. Its leaves have attracted increasing attention as a potential natural resource because previous studies have reported multiple biological activities of *P. koraiensis* leaf-derived preparations, including antioxidant, anti-inflammatory, anticancer, anti-obesity, antidiabetic, antihyperlipidemic, and anti-fatigue effects [1-5]. In particular, recent studies have investigated *P. koraiensis* leaf materials prepared by extractive methods, such as leaf extracts, essential oils, and supercritical CO_2-extracted oils, and demonstrated their bioactivities in several experimental models. However, these preparations differ from food-compatible pressed juice materials, which may be more suitable for beverage-type functional food applications. Plant-derived phenolic compounds and flavonoids are major contributors to antioxidant activity because they can scavenge free radicals and participate in cellular redox regulation. Radical scavenging assays such as DPPH and ABTS are widely used to estimate the antioxidant potential of natural products, although their results should be interpreted together with phytochemical contents and cellular functional assays because each assay reflects different reaction mechanisms [6]. Therefore, evaluating total polyphenol content, flavonoid content, and cellular antioxidant responses provides a more comprehensive assessment of functional food materials than chemical antioxidant assays alone. Coconut water (CW) is a natural beverage matrix containing sugars, minerals, amino acids, organic acids, and phenolic compounds, and its nutritional composition and biological activities have been reviewed in relation to hydration, antioxidant potential, and food processing applications [7-8]. Previous studies have also shown that coconut water contains measurable phenolic compounds and exhibits antioxidant activity, although the levels vary depending on coconut maturity, variety, and processing conditions [8]. Based on these characteristics, CW may serve not only as a palatable beverage base but also as a formulation matrix that could modify the dispersion, stability, or measurable recovery of phytochemicals from plant-derived materials. Oxidative stress and inflammation are closely linked biological processes involved in hepatic and intestinal

epithelial dysfunction. Nuclear factor erythroid 2-related factor 2 (Nrf2) is a key transcription factor that regulates cytoprotective antioxidant responses, including glutathione-related redox defense pathways [9-13]. In HepG2 cells, hydrogen peroxide (H_2O_2) is widely used to induce oxidative stress-mediated hepatocellular injury, characterized by increased reactive oxygen species, altered glutathione redox balance, reduced antioxidant enzyme activity, and activation of oxidative inflammatory signaling [14-17]. Thus, the H_2O_2-induced HepG2 model provides a useful in vitro system for evaluating antioxidant and hepatoprotective potential. In addition to oxidative stress, fructose overload has been used to induce metabolic and lipogenic stress responses in HepG2 cells. Previous studies reported that fructose treatment can increase triglyceride accumulation and upregulate lipogenesis-related factors, including sterol regulatory element-binding protein-1c (SREBP-1c) and fatty acid synthase (FAS), although fructose-induced responses in HepG2 cells may vary depending on culture conditions and experimental design [18-22]. Macrophage-mediated inflammation is another important target for evaluating functional food materials. Lipopolysaccharide (LPS)-stimulated THP-1 cells are commonly used as an in vitro inflammatory model, in which LPS induces pro-inflammatory mediators such as inducible nitric oxide synthase (iNOS), nitric oxide (NO), tumor necrosis factor-α (TNF-α), and interleukin-6 (IL-6) [23-27]. Therefore, suppression of iNOS/NO production and pro-inflammatory cytokine expression in LPS-stimulated THP-1 cells can provide evidence for anti-inflammatory activity. The intestinal epithelium is a critical barrier that regulates nutrient absorption, host-microbiota interactions, and protection against luminal stressors. Tight junction proteins, including zonula occludens-1 (ZO-1) and claudins, are essential for maintaining epithelial barrier integrity [28-33]. Oxidative stress can disrupt epithelial tight junctions, and H_2O_2-treated Caco-2 cells have been widely used as an in vitro model of oxidative intestinal epithelial injury and barrier dysfunction [33-36]. In addition, Caco-2 cells have been used as a human intestinal epithelial model to examine glucagon-like peptide-1 (GLP-1)-related responses, although GLP-1 findings in this cell line should be interpreted as epithelial functional responses rather than complete enteroendocrine physiology [37-39]. In the present study, we developed a pressed Korean pine leaf juice/coconut water mixed formulation, designated PC, as a functional food-compatible material for functional beverage applications. Unlike previously studied

P. koraiensis leaf preparations obtained through ethanol or oil extraction, PKJ was prepared by aqueous homogenization and pressing, and CW was incorporated as a beverage-type mixed formulation. The PKJ formulation ratio was selected through antioxidant-based formulation screening, while the concentration range used for subsequent cellular experiments was determined from antioxidant activity and total polyphenol and flavonoid profiles. To provide hypothesis-generating mechanistic context, a literature-based network analysis was performed using phytochemicals previously reported in *P. koraiensis* and *C. nucifera*. The biological effects of the selected PC formulation were then evaluated in LPS-stimulated THP-1 cells, H_2O_2- and fructose-treated HepG2 cells, and H_2O_2-treated Caco-2 cells to investigate its anti-inflammatory, antioxidant, metabolic stress-modulating, and intestinal epithelial protective potential.

2. Materials and Methods

2.1. Preparation of pressed Korean pine leaf juice (PKJ) and PKJ-coconut beverage (PC)

Fresh *P. koraiensis* leaves were purchased from the Duwibong Farming Association Corporation (Jeongseon, Gangwon-do, South Korea) in 2025. The leaves (500 g) were thoroughly washed and homogenized with distilled water at a 1:2 (w/v) ratio using a blender (DA282-2, Artlon, Gyeonggi-do, South Korea), followed by juice extraction using a juicer (CS700KC, NUC, Daegu, South Korea). The resulting juice was centrifuged at 1,000 rpm for 3 min, and the supernatant was collected as pressed Korean pine leaf juice (PKJ). For heat-treated samples, PKJ was heated at 100 °C for 15 min as a laboratory-scale thermal processing step prior to formulation. The PKJ-coconut formulation (PC) was prepared using coconut water (CW) (Nam Viet Foods and Beverage JSC, Vietnam). The formulation ratio was selected on the basis of preliminary antioxidant screening. Because the 1:9 formulation retained antioxidant activity comparable to that of the 1:1 formulation while containing a lower proportion of PKJ, the 1:9 ratio was selected for subsequent functional evaluation. PC was therefore prepared by mixing 10% (v/v) PKJ with 90% (v/v) CW.

2.2. Total Phenolic Content

The total phenolic content (TPC) of each sample was determined using the Folin-Ciocalteu method [40] with slight modifications. Gallic acid was used as the standard compound for calibration. Briefly, 50 µL of each sample was added in triplicate to a 96-well plate (SPL Life Sciences, Pocheon, South Korea), followed by the addition of 50 µL of Folin-Ciocalteu reagent and incubation at room temperature for 10 min. Subsequently, 50 µL of 10% (w/w) sodium carbonate solution was added, and the mixture was further incubated at room temperature for 1 h. Absorbance was measured at 765 nm using a microplate reader (Thermo Fisher Scientific, Waltham, MA, USA). TPC was calculated using a gallic acid standard curve (0-1000 µg/mL) and expressed as µg gallic acid equivalents (GAE)/mL of fresh sample.

2.3. Total Flavonoid Content

The total flavonoid content (TFC) of each sample was determined according to the method of Davis [41] with slight modifications. Quercetin and catechin were used as reference standards for calibration. Briefly, 50 µL of each sample was added in triplicate to a 96-well plate. Subsequently, 50 µL of 90% diethylene glycol and 50 µL of 1 N NaOH were added to each well. The mixture was incubated at room temperature for 1 h, and absorbance was measured at 420 nm using a microplate reader (Thermo Fisher Scientific, Waltham, MA, USA). TFC was calculated using quercetin and catechin standard curves (0-1000 µg/mL) and expressed as µg quercetin equivalents (QE)/mL and µg catechin equivalents (CE)/mL of fresh sample, respectively.

2.4. DPPH Radical Scavenging Activity

The DPPH radical scavenging activity was determined according to the method of Blois [42]. Briefly, 100 µL of each sample was mixed with 100 µL of 0.2 mM DPPH solution (1,1-diphenyl-2-picrylhydrazyl; Sigma-Aldrich, St. Louis, MO, USA) in a 96-well plate. The reaction mixture was incubated in the dark at room temperature for 30 min. Absorbance was measured at 517 nm using a microplate reader (Thermo Fisher Scientific, Waltham, MA, USA). Ascorbic acid (0-1000 µg/mL) was used to generate the standard curve. The radical scavenging activity (RSA) was calculated and expressed as ascorbic acid equivalent antioxidant capacity (AEAC).

2.5. ABTS Radical Scavenging Activity

The ABTS radical scavenging activity was determined according to the method of Verzelloni et al. [43]. ABTS radical cations were generated by mixing 7.4 mM ABTS solution [2,2′-azino-bis(3-ethylbenzothiazoline-6-sulfonic acid); Sigma-Aldrich, St. Louis, MO, USA] with 2.7 mM potassium persulfate solution at a 1:1 ratio, followed by incubation in the dark at room temperature for 14 h. The ABTS solution was diluted with 50% methanol to obtain an absorbance of 0.7-0.8 at 734 nm. Briefly, 100 μL of each sample was mixed with 100 μL of the ABTS solution in a 96-well plate and incubated for 30 min at room temperature. Absorbance was measured at 734 nm using a microplate reader (Thermo Fisher Scientific, Waltham, MA, USA). Ascorbic acid (0-1000 μg/mL) was used to generate the standard curve. The radical scavenging activity (RSA) was calculated and expressed as ascorbic acid equivalent antioxidant capacity (AEAC).

2.6. Synergy Analysis

The interaction between PKJ and CW was evaluated using the SynergyFinder platform. Various concentration combinations of PKJ and CW were prepared in a matrix format, and antioxidant response values were converted to the response format required for synergy analysis. Synergy Scores were calculated using the Zero Interaction Potency (ZIP) model. Positive ZIP scores were interpreted as evidence of a greater-than-expected combined antioxidant response. The synergy analysis was used as one component of the formulation-selection process together with direct antioxidant activity measurements.

2.7. Bioinformatics Analysis

The bioactive compounds of *P. koraiensis* and *C. nucifera* were identified based on previously published studies. Shared phytochemicals reported in both species were analyzed using the Comparative Toxicogenomics Database (CTD) to identify compound-associated target genes. Disease-associated genes related to inflammation, oxidative stress, non-alcoholic fatty liver disease, diabetes, and chronic colitis were collected using the GeneShot database. Overlapping genes among the disease-associated

gene sets and compound-associated targets were subsequently identified. Protein-Protein Interaction (PPI) networks of the overlapping targets were analyzed using the STRING database to identify candidate molecular nodes potentially relevant to the subsequent cellular experiments.

2.8. Cell Culture

The human monocytic leukemia cell line THP-1 (Cat. No. 40202, Korean Cell Line Bank, Seoul, South Korea), human hepatocellular carcinoma cell line HepG2 (Cat. No. HB-8065, ATCC, Manassas, VA, USA), and human colorectal adenocarcinoma cell line Caco-2 (Cat. No. 30037.1, Korean Cell Line Bank, Seoul, South Korea) were used in this study. THP-1 cells were cultured in Roswell Park Memorial Institute (RPMI)-1640 medium (Cat. No. LM011-01, WELGENE, Daegu, South Korea) supplemented with 10% fetal bovine serum (FBS) and 1% antibiotic solution. HepG2 cells were cultured in Dulbecco's Modified Eagle Medium (DMEM; Cat. No. LM001-01, WELGENE, Daegu, South Korea) supplemented with 10% FBS and 1% antibiotic solution. Caco-2 cells were cultured in Minimum Essential Medium (MEM; Cat. No. LM007-01, WELGENE, Daegu, South Korea) supplemented with 10% FBS and 1% antibiotic solution. All cells were maintained at 37 °C in a humidified incubator containing 5% CO_2.

2.9. Cell Viability Assay

THP-1, HepG2, and Caco-2 cells were seeded into 96-well plates at a density of 2×10^4 cells/well and incubated for 24 h. The cells were then treated with various concentrations of PC (0.16-10%), H_2O_2 (12.5-800 μM; Duksan Pure Chemicals, Gyeonggi-do, South Korea), or D-(−)-fructose (0.3-20 mM; Sigma-Aldrich, St. Louis, MO, USA) for an additional 24 h. Cell viability was evaluated using a CELLOMAX cell viability kit (Precaregene, Gyeonggi-do, South Korea) according to the manufacturer's instructions. Briefly, 10 μL of CELLOMAX reagent was added to each well, followed by incubation in the dark for 1 h at 37°C. The absorbance was measured at 450 nm using a microplate reader (Tecan Sunrise, Männedorf, Switzerland), and cell viability was determined as previously described [44]. Cell viability was expressed as a percentage relative to the untreated control group.

2.10. Nitric Oxide (NO) Production Assay

NO production was evaluated using the Griess method [45]. THP-1 cells (1×10^6 cells), HepG2 cells (5×10^5 cells), and Caco-2 cells (4×10^5 cells) were seeded into 6-well plates (SPL Life Sciences, Gyeonggi-do, South Korea). THP-1 cells were treated with LPS (1 μg/mL) in the presence or absence of PC (0.625%, 1.25%, or 2.5%). HepG2 and Caco-2 cells were treated with H_2O_2 (200 μM and 100 μM, respectively) in the presence or absence of PC for 24 h. After incubation, 50 μL of culture supernatant was mixed with nitrate and sulfanilamide solutions, and the reaction mixture was incubated in the dark for 10 min. Absorbance was measured at 570 nm using a microplate reader (Tecan, Männedorf, Switzerland).

2.11. Glutathione (GSH/GSSG, Total) Assay

HepG2 cells (5×10^5 cells) and Caco-2 cells (4×10^5 cells) were seeded into 6-well plates and incubated for 24 h. The cells were treated with H_2O_2 (200 μM and 100 μM, respectively) in the presence or absence of PC (0.625%, 1.25%, or 2.5%) for 24 h. Total glutathione (GSH/GSSG) levels were measured using an EZ-Glutathione Assay Kit (DE-GLU200, DoGenBio Co., Ltd., Seoul, South Korea) according to the manufacturer's instructions. Briefly, 50 μL of standards, blanks, and samples were added to 96-well plates, followed by the addition of 50 μL of chromogen (DTNB) and 50 μL of enzyme solution (GR) to each well. After incubation at room temperature for 5 min, 50 μL of NADPH solution was added. Absorbance was measured kinetically at 412 nm for 3 min at intervals of 30 s or less using a microplate reader (Tecan, Männedorf, Switzerland).

2.12. RNA Isolation and qRT-PCR

THP-1 cells (1×10^6 cells), HepG2 cells (5×10^5 cells), and Caco-2 cells (4×10^5 cells) were seeded into 6-well plates and incubated for 24 h. THP-1 cells were treated with LPS (1 μg/mL) in the presence or absence of PC (0.625%, 1.25%, or 2.5%). HepG2 and Caco-2 cells were treated with H_2O_2 (200 μM and 100 μM, respectively) in the presence or absence of PC for 24 h. Total RNA was isolated using TRIzol™ Reagent (Cat. No. 15596026, Invitrogen™, Carlsbad, CA, USA). Complementary DNA

(cDNA) was synthesized using a High-Capacity cDNA Reverse Transcription Kit (M1701, Promega, Madison, WI, USA). Quantitative real-time PCR was performed using a SYBR Green RT-PCR kit (Bioneer, Seoul, South Korea). The primer sequences used for qRT-PCR are listed in Table 1. Gene expression was analyzed for inducible nitric oxide synthase (iNOS), glucagon-like peptide-1 (GLP-1), glutamate-cysteine ligase catalytic subunit (GCLC), glutamate-cysteine ligase modifier subunit (GCLM), glutathione synthetase (GSS), and β-actin. Amplification and analysis were conducted using the Thermal Cycler Dice® Real-Time System III (Takara Bio Inc., Shiga, Japan). Relative gene expression levels were normalized to β-actin using the $2^{-\Delta\Delta Ct}$ method.

Table 1. Primer sequences used in this study.

Gene	Forward primer	Reverse primer
iNOS	GCTCTACACCTCCAATGTGACC	CTGCCGAGATTTGAGCCTCATG
GLP-1	CGTTCCCTTCAAGACACAGAGG	ACGCCTGGAGTCCAGATACTTG
GCLC	GGAAGTGGATGTGGACACCAGA	GCTTGTAGTCAGGATGGTTTGCG
GCLM	TCTTGCCTCCTGCTGTGTGATG	TTGGAAACTTGCTTCAGAAAGCAG
GSS	CCAAGACCGAAGGCTGTTTGTG	TGTGACCTCTCCAGCAGTAGAC
β-actin	CACCATTGGCAATGAGCGGTTC	AGGTCTTTGCGGATGTCCACGT

2.13. Western Blot Analysis

THP-1 cells (1×10^6 cells), HepG2 cells (5×10^5 cells), and Caco-2 cells (4×10^5 cells) were seeded into 6-well plates and incubated for 24 h. THP-1 cells were treated with LPS (1 μg/mL) in the presence or absence of PC (0.625%, 1.25%, or 2.5%). HepG2 cells were treated with H_2O_2 (200 μM)

or fructose (10 mM) in the presence or absence of PC for 24 h, whereas Caco-2 cells were treated with H_2O_2 (100 μM) in the presence or absence of PC for 24 h. Cells were lysed using RIPA buffer containing 50 mM Tris-HCl (pH 7.4), 150 mM NaCl, 1% NP-40, 0.25% sodium deoxycholate, 1 mM EDTA, 1 mM Na_3VO_4, 1 mM NaF, and protease inhibitor cocktail. Protein concentrations were determined using the DC™ Protein Assay Kit II (Cat. No. 5000112, Bio-Rad, Hercules, CA, USA). Equal amounts of protein were separated on 6-15% SDS-PAGE gels and transferred onto Hybond ECL nitrocellulose membranes (Cat. Nos. 10600002 and 10600001, Amersham Pharmacia, Piscataway, NJ, USA). Membranes were blocked with 5% non-fat dry milk (Cat. No. 232100, BD, Franklin Lakes, NJ, USA) for 1 h at room temperature and incubated overnight at 4°C with primary antibodies (Table 2). After washing, membranes were incubated with horseradish peroxidase (HRP)-conjugated anti-mouse or anti-rabbit secondary antibodies. Protein bands were visualized using an enhanced chemiluminescence (ECL) detection system (Cat. No. RPN2209, Amersham Pharmacia, Piscataway, NJ, USA).

Table 2. Antibodies used in this study.

Antibody	Company	Dilution	Product No.
iNOS	Aviva	1:1000	OAED00107
ZO-1	Cell Signaling	1:1000	D7D12
Claudin-1	Cell Signaling	1:1000	D5H1D
Nrf2	Santa Cruz	1:1000	sc-365949
FAS	Cell Signaling	1:1000	C20G5
SREBP-1	Santa Cruz	1:1000	sc-365513

TNF-α	Santa Cruz	1:1000	sc-52746
IL-6	Santa Cruz	1:1000	sc-28343
β-actin	Sigma-Aldrich	1:20,000	A5316
Goat anti-rabbit IgG (HRP)	Jackson	1:5000	111-035-003
Goat anti-mouse IgG (HRP)	Jackson	1:5000	115-035-003

Aviva Systems Biology (San Diego, CA, USA); Cell Signaling Technology (Danvers, MA, USA); Santa Cruz Biotechnology (Dallas, TX, USA); Sigma-Aldrich (St. Louis, MO, USA); Jackson ImmunoResearch (West Grove, PA, USA).

2.14. Statistical Analysis

The data are presented as mean ± standard deviation (SD) from three independent experiments. Statistical analyses were conducted using one-way analysis of variance (ANOVA) followed by Duncan's multiple range test using SigmaPlot software (version 14.0; Systat Software Inc., San Jose, CA, USA). Different letters (a-c) indicate significant differences among groups ($p < 0.05$). The symbol # indicates a significant difference compared with the control group, whereas * indicates a significant difference compared with the LPS-, H_2O_2-, or fructose-treated group (#/*$p < 0.05$, ##/**$p < 0.01$, ###/***$p < 0.001$).

3. Results

3.1 Determination of the selected PC formulation based on antioxidant activity and phytochemical characteristics

The antioxidant properties of PKJ, CW, and their mixed formulation PC were first evaluated to establish an appropriate formulation for subsequent functional studies. PKJ showed concentration-dependent DPPH and ABTS radical scavenging activities, whereas CW alone exhibited minimal antioxidant activity (Figure 1a and b). PC consistently showed greater antioxidant responses than either PKJ or CW

alone. Consistent with these observations, PC exhibited higher total polyphenol and flavonoid assay values than the individual components (Figure 1c-e). ZIP analysis further indicated a positive interaction between PKJ and CW across the tested concentration combinations, with a mean synergy score of 16.15 (p=0.00000681) (Figure 1f). Comparison of 1:1 and the 1:9 PKJ formulations showed comparable antioxidant activity (Figure 1g). Because the 1:9 formulation retained antioxidant performance despite containing a substantially lower proportion of PKJ, this ratio was selected as the PC formulation for subsequent experiments. The selected 1:9 formulation was subsequently evaluated at 0.625%, 1.25%, and 2.5%. PC showed greater DPPH and ABTS antioxidant responses than PKJ or CW alone across these concentrations (Figure 1h and i). Similarly, total polyphenol and flavonoid assay values were significantly higher in PC than in the components (Figure 1j-l). Together, these findings provided the basis for selecting the 1:9 formulation and the concentration range used in subsequent cellular assays.

3.2 Network-based pharmacology analysis suggested potential molecular targets associated with PC-related compounds

Following selection of the PC formulation, a network pharmacology-based analysis was performed to explore the potential molecular targets underlying its biological activity. Phytochemicals previously reported in *P. koraiensis* and *C. nucifera* were collected, and their putative target genes were compared with disease-associated gene sets related to inflammation, oxidative stress, non-alcoholic fatty liver, diabetes, and chronic colitis (Figure 2a). Gallic acid, catechin, and epicatechin were identified as phytochemicals reported in both plant sources (Figure 2b). Target prediction of these shared compounds identified overlapping genes associated with inflammatory and oxidative stress responses, including IL-6, IL-1β, BCL-2, CASP3, AKT1, MAPK1, PTGS2 and NOS2 (Figure 2c). Comparisons with disease-associated gene sets further identified shared molecular targets across inflammation, oxidative stress, non-alcoholic fatty liver disease, diabetes, and chronic colitis (Figure 2d-h). Integrated analysis identified BCL2, CASP3, HMOX1, IL6, NFE2L2, and NOS2 as common candidate targets (Figure 2i-k). These results were considered hypothesis-generating and provided a molecular framework for

interpreting the subsequent cellular experiments rather than direct evidence of the chemical composition of PC.

3.3 Anti-inflammatory effects of PC in LPS-stimulated THP-1 cells

The PC concentration range used in the functional assays was selected from the antioxidant and phytochemical screening described above. Cell viability was examined in THP-1 cells to verify that the concentrations used for subsequent experiments did not produce substantial nonspecific cytotoxicity. PC showed no marked reduction in cell viability at the lower concentrations used for mechanistic evaluation, although modest decreases were observed at higher concentrations (Figure 3a). LPS stimulation significantly increased iNOS expression compared with untreated control cells (Figure 3b). However, treatment with PC reduced LPS-induced iNOS expression in a concentration-dependent manner. Consistently, LPS markedly increased nitric oxide production, whereas PC treatment significantly suppressed NO levels in LPS-stimulated THP-1 cells (Figure 3c). Western blot analysis further showed that LPS increased the expression of iNOS, TNF-α, and IL-6, whereas PC treatment attenuated the upregulation of these inflammatory mediators (Figure 3d). In contrast, PC treatment attenuated the LPS-induced upregulation of these proteins. These findings indicate that PC suppresses LPS-induced inflammatory responses in THP-1 cells, including the iNOS/NO axis and pro-inflammatory cytokine expression.

3.4 Protective effects of PC against H_2O_2-induced oxidative stress and fructose-induced metabolic stress in HepG2 cells

To evaluate the hepatoprotective potential of PC, HepG2 cells were exposed to H_2O_2 to establish an in vitro oxidative stress-mediated hepatocellular injury model. Cell viability analysis confirmed that the PC concentrations used for subsequent mechanistic studies did not cause substantial cytotoxicity, while H_2O_2 progressively reduced HepG2 cell viability (Figure 4a and b). H_2O_2 exposure significantly reduced the expression levels of glutamate-cysteine ligase catalytic subunit (GCLC), glutamate-cysteine ligase modifier subunit (GCLM), and glutathione synthetase (GSS), indicating impairment of the glutathione-

dependent antioxidant defense system (Figure 4c-e). However, PC treatment markedly restored the expression of these antioxidant-related genes in a concentration-dependent manner. Consistently, the GSH/GSSG ratio, which was substantially decreased by H_2O_2 treatment, was significantly recovered by PC treatment (Figure 4f). H_2O_2 also increased iNOS expression and NO production, whereas PC attenuated both responses (Figure 4g and h). In addition, H_2O_2 reduced Nrf2 protein expression, which was partially restored by PC treatment (Figure 4i). The protective effect of PC was further examined under fructose-induced metabolic stress conditions. Fructose increased the expression of lipogenesis-related proteins fatty acid synthase (FAS) and sterol regulatory element-binding protein 1 (SREBP-1), and increased iNOS expression compared with untreated cells. PC treatment progressively attenuated these fructose-induced changes (Figure 4j). These results suggest that PC suppresses fructose-induced metabolic stress by suppressing both lipogenic and inflammatory responses in HepG2 cells.

3.5 Protective effects of PC against H_2O_2-induced oxidative intestinal epithelial injury in Caco-2 cells

We next investigated whether the protective effects of PC extended to intestinal epithelial cells using an H_2O_2-induced Caco-2 oxidative injury model. Cell viability analysis confirmed that the PC concentrations used for functional experiments did not cause substantial nonspecific cytotoxicity, whereas increasing H_2O_2 concentrations progressively reduced Caco-2 cell viability (Figure 5a and b). H_2O_2 exposure significantly decreased the expression levels of GCLC, GCLM, and GSS, which are key enzymes involved in glutathione biosynthesis and redox regulation (Figure 5c-e). In contrast, PC treatment restored the expression of these antioxidant defense-related genes in a concentration-dependent manner. Consistently, the GSH/GSSG ratio, which was markedly reduced by H_2O_2 exposure, was significantly recovered following PC treatment (Figure 5f). These results indicate that PC enhances glutathione-dependent antioxidant defense and restores intracellular redox balance in H_2O_2-stimulated Caco-2 cells. We then examined whether the restoration of antioxidant defense was accompanied by suppression of oxidative inflammatory responses. H_2O_2 markedly increased iNOS expression and nitric oxide production, whereas PC treatment significantly suppressed these increases (Figure 5g and h). In

addition, H_2O_2 reduced GLP-1 expression, while PC treatment restored GLP-1 levels, suggesting that PC may help preserve intestinal epithelial functional responses under oxidative stress conditions (Figure 5i). Finally, the effect of PC on epithelial barrier-related proteins was assessed. H_2O_2 reduced the expression of the tight junction–associated proteins ZO-1 and claudin-1, whereas PC treatment restored their expression in Caco-2 cells (Figure 5j). These findings suggest that PC may contribute to the preservation of intestinal epithelial barrier integrity under oxidative stress conditions. Collectively, these results demonstrate that PC protects Caco-2 cells against H_2O_2-induced oxidative epithelial injury by restoring glutathione-dependent antioxidant defense, suppressing iNOS/NO-mediated oxidative inflammatory responses, and preserving epithelial barrier-associated proteins.

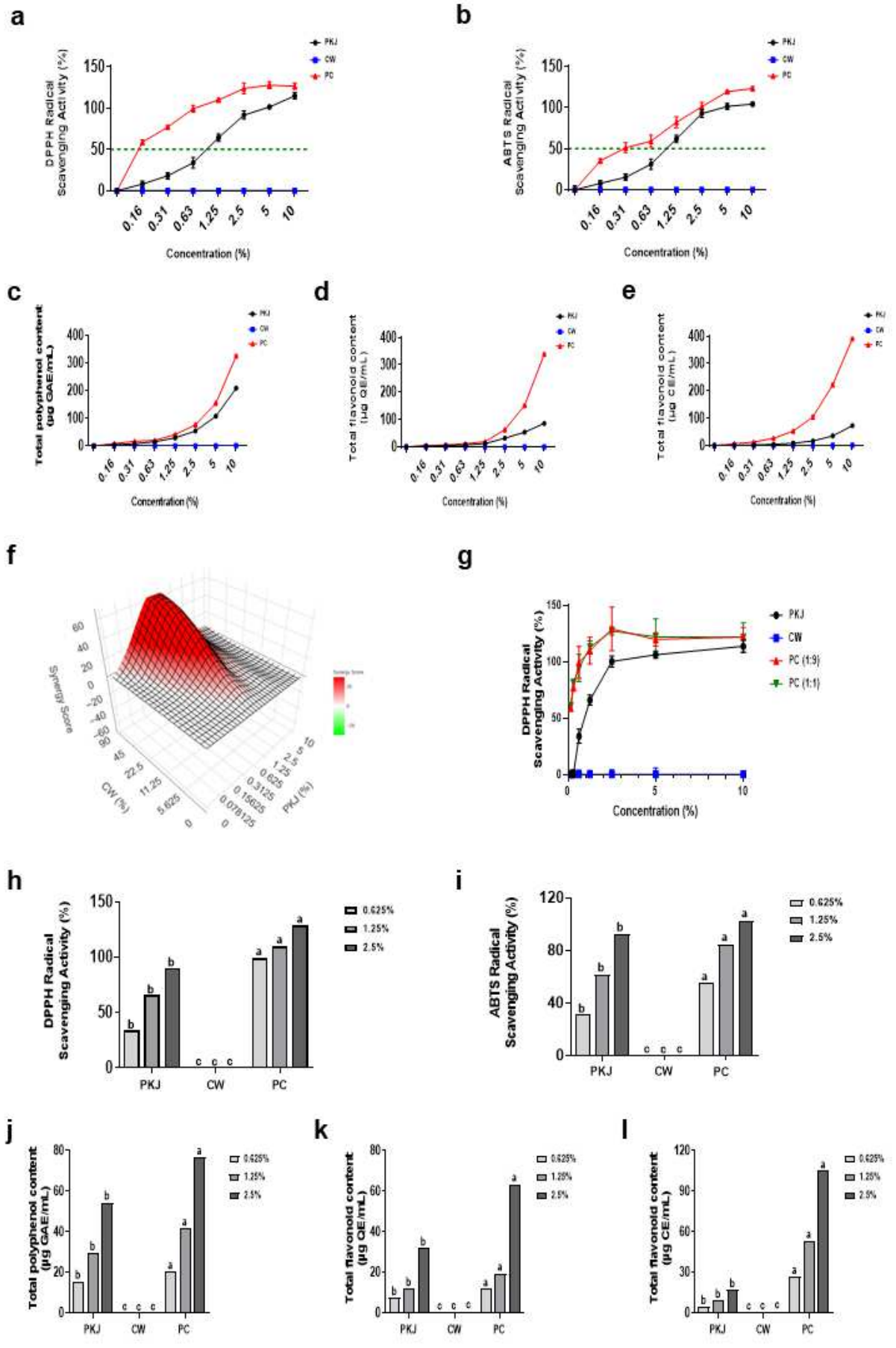

a
DPPH Radical Scavenging Activity (%)
PKJ
CW
PC
Concentration (%)
b
ABTS Radical Scavenging Activity (%)
c
Total polyphenol content (µg GAE/mL)
d
Total flavonoid content (µg QE/mL)
e
Total flavonoid content (µg CE/mL)
f
Synergy Score
CW (%)
PKJ (%)
g
PC (1:9)
PC (1:1)
h
0.625%
1.25%
2.5%
i
j
k
l

Figure 1. Optimization of the PKJ-coconut beverage formulation based on antioxidant activity, phytochemical content, and synergy analysis. (a) DPPH radical scavenging activity and (b) ABTS radical scavenging activity of PKJ, CW, and PC formulations at different mixing ratios; (c) total polyphenol content expressed as gallic acid equivalents, (d) total flavonoid content expressed as quercetin equivalents, and (e) total flavonoid content expressed as catechin equivalents of PKJ, CW, and PC formulations; (f) SynergyFinder analysis showing the interaction between PKJ and CW, with a mean ZIP synergy score of 16.15; (g) comparison of antioxidant activity between the 1:1 and 1:9 PKJ formulations used for formulation selection; (h) DPPH radical scavenging activity and (i) ABTS radical scavenging activity of PKJ, CW, and the selected 1:9 PC formulation at 0.625%, 1.25%, and 2.5%; (j) total polyphenol content expressed as gallic acid equivalents, (k) total flavonoid content expressed as quercetin equivalents, and (l) total flavonoid content expressed as catechin equivalents of PKJ, CW, and PC at 0.625%, 1.25%, and 2.5%. Data are presented as the mean ± SD of three independent experiments. Statistical analyses were performed using one-way analysis of variance (ANOVA) followed by Duncan's multiple range test. Different letters (a-c) indicate significant differences among groups ($p < 0.05$).

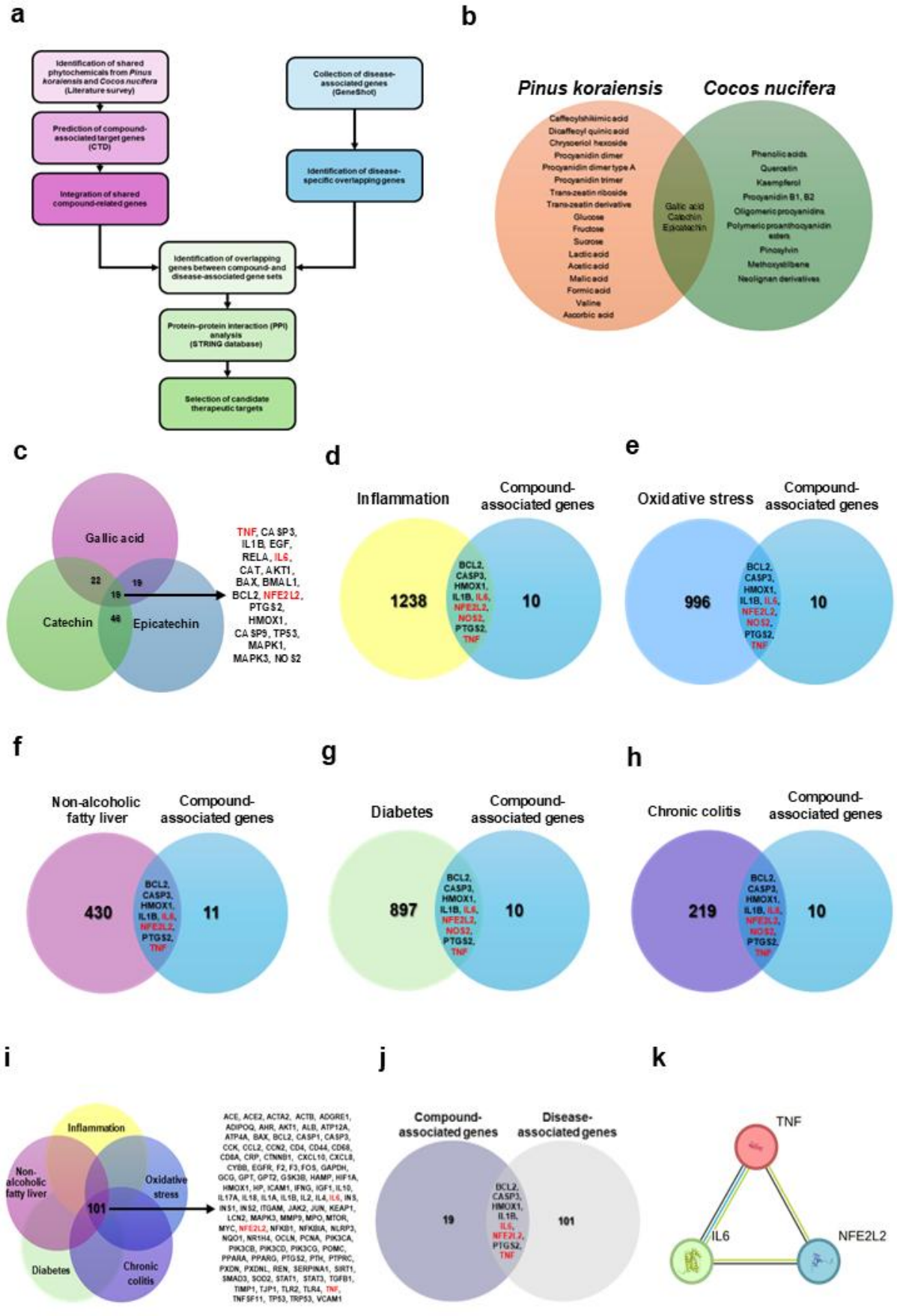
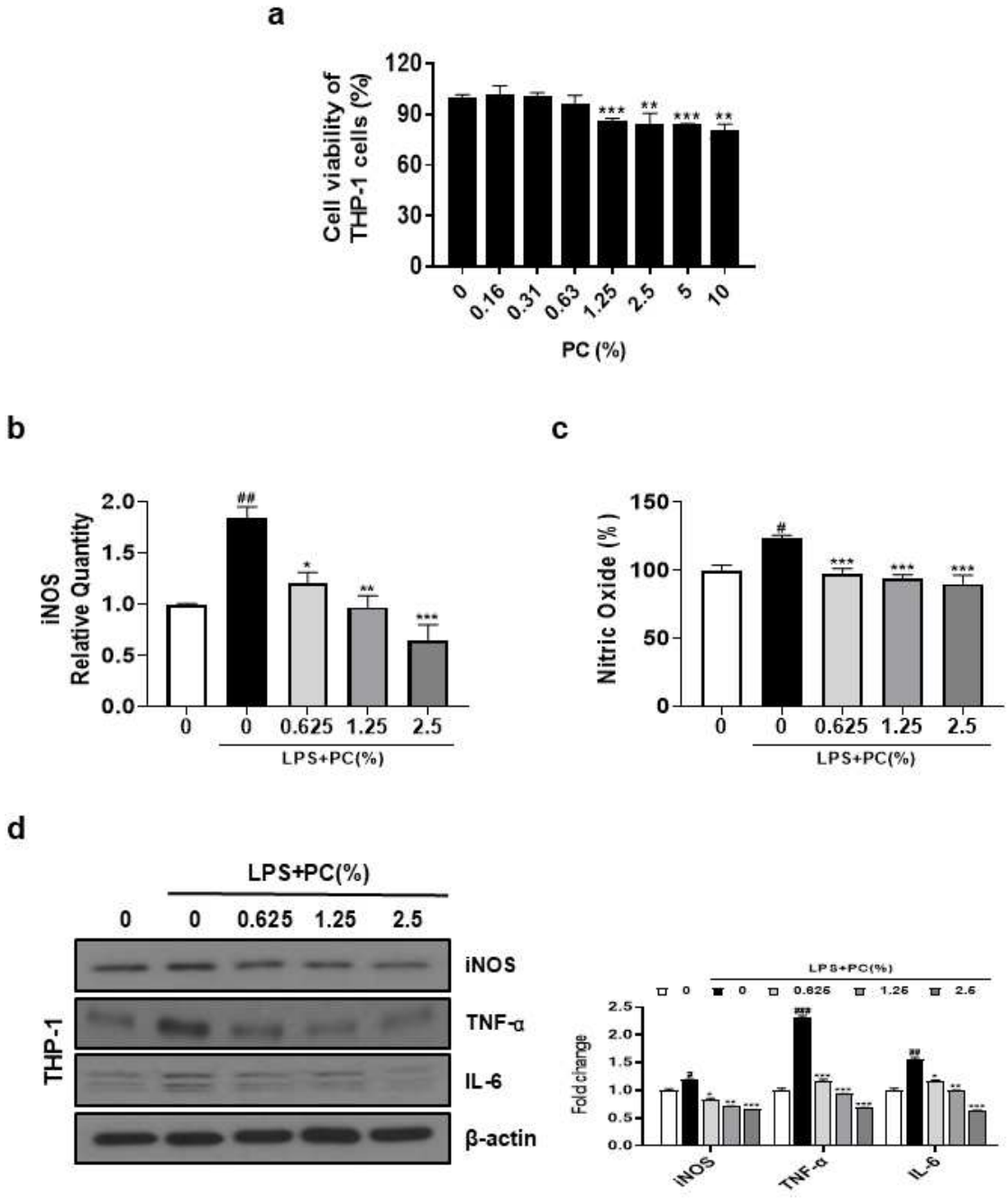

a
Identification of shared phytochemicals from Pinus koraiensis and Cocos nucifera (Literature survey)
Prediction of compound-associated target genes (CTD)
Integration of shared compound-related genes
Collection of disease-associated genes (GeneShot)
Identification of disease-specific overlapping genes
Identification of overlapping genes between compound- and disease-associated gene sets
Protein-protein interaction (PPI) analysis (STRING database)
Selection of candidate therapeutic targets
b
Pinus koraiensis
Cocos nucifera
Caffeoylshikimic acid
Dicaffeoyl quinic acid
Chrysoeriol hexoside
Procyanidin dimer
Procyanidin dimer type A
Procyanidin trimer
Trans-zeatin riboside
Trans-zeatin derivative
Glucose
Fructose
Sucrose
Lactic acid
Acetic acid
Malic acid
Formic acid
Valine
Ascorbic acid
Gallic acid
Catechin
Epicatechin
Phenolic acids
Quercetin
Kaempferol
Procyanidin B1, B2
Oligomeric procyanidins
Polymeric proanthocyanidin esters
Pinosylvin
Methoxystilbene
Neolignan derivatives
c
Gallic acid
Catechin
Epicatechin
22
19
19
46
TNF, CASP3, IL1B, EGF, RELA, IL6, CAT, AKT1, BAX, BMAL1, BCL2, NFE2L2, PTGS2, HMOX1, CASP9, TP53, MAPK1, MAPK3, NOS2
d
Inflammation
Compound-associated genes
1238
BCL2, CASP3, HMOX1, IL1B, IL6, NFE2L2, NOS2, PTGS2, TNF
10
e
Oxidative stress
Compound-associated genes
996
BCL2, CASP3, HMOX1, IL1B, IL6, NFE2L2, NOS2, PTGS2, TNF
10
f
Non-alcoholic fatty liver
Compound-associated genes
430
BCL2, CASP3, HMOX1, IL1B, IL6, NFE2L2, PTGS2, TNF
11
g
Diabetes
Compound-associated genes
897
BCL2, CASP3, HMOX1, IL1B, IL6, NFE2L2, NOS2, PTGS2, TNF
10
h
Chronic colitis
Compound-associated genes
219
BCL2, CASP3, HMOX1, IL1B, IL6, NFE2L2, NOS2, PTGS2, TNF
10
i
Inflammation
Non-alcoholic fatty liver
Oxidative stress
Diabetes
Chronic colitis
101
ACE, ACE2, ACTA2, ACTB, ADGRE1, ADIPOQ, AHR, AKT1, ALB, ATP12A, ATP4A, BAX, BCL2, CASP1, CASP3, CCK, CCL2, CCN2, CD4, CD44, CD68, CD8A, CRP, CTNNB1, CXCL10, CXCL8, CYBB, EGFR, F2, F3, FOS, GAPDH, GCG, GPT, GPT2, GSK3B, HAMP, HIF1A, HMOX1, HP, ICAM1, IFNG, IGF1, IL10, IL17A, IL18, IL1A, IL1B, IL2, IL4, IL6, INS, INS1, INS2, ITGAM, JAK2, JUN, KEAP1, LCN2, MAPK3, MMP9, MPO, MTOR, MYC, NFE2L2, NFKB1, NFKBIA, NLRP3, NQO1, NR1H4, OCLN, PCNA, PIK3CA, PIK3CB, PIK3CD, PIK3CG, POMC, PPARA, PPARG, PTGS2, PTH, PTPRC, PXDN, PXDNL, REN, SERPINA1, SIRT1, SMAD3, SOD2, STAT1, STAT3, TGFB1, TIMP1, TJP1, TLR2, TLR4, TNF, TNFSF11, TP53, TRP53, VCAM1
j
Compound-associated genes
Disease-associated genes
19
BCL2, CASP3, HMOX1, IL1B, IL6, NFE2L2, PTGS2, TNF
101
k
TNF
IL6
NFE2L2

Figure 2. Network pharmacology analysis identifying potential molecular targets associated with PC-derived compounds. (a) Schematic workflow of the network pharmacology analysis used to identify shared target genes associated with compounds derived from Pinus koraiensis and Cocos nucifera and disease-related gene sets; (b) Venn diagram showing common phytochemicals identified between P. koraiensis and C. nucifera; (c) overlapping target genes predicted from the shared phytochemicals; (d-h) overlap analyses between compound-associated target genes and disease-associated genes related to (d) inflammation, (e) oxidative stress, (f) non-alcoholic fatty liver, (g) diabetes, and (h) chronic colitis; (i) Venn diagram showing common disease-associated genes identified among inflammation, oxidative stress, non-alcoholic fatty liver, diabetes, and chronic colitis; (j) integrated overlap analysis identifying common molecular targets shared between PC-associated compounds and disease-related gene sets; (k) STRING-based interaction network analysis of the overlapping core genes.



361

362 **Figure 3.** Anti-inflammatory effects of PC in LPS-stimulated THP-1 cells. (a) Cell viability of THP-1
363 cells treated with PC; (b) relative iNOS mRNA expression in THP-1 cells stimulated with 1 μg/mL LPS
364 and treated with PC; (c) nitric oxide (NO) production in THP-1 cells; (d) Western blot analysis of iNOS,
365 TNF-α, and IL-6 protein expression in THP-1 cells. Data are presented as the mean ± SD of three
366 independent experiments. The symbol # indicates significant differences compared with the untreated
367 control group, whereas * indicates significant differences compared with the LPS-treated group (#/**p*

< 0.05, ##/**p < 0.01, ###/***p < 0.001).

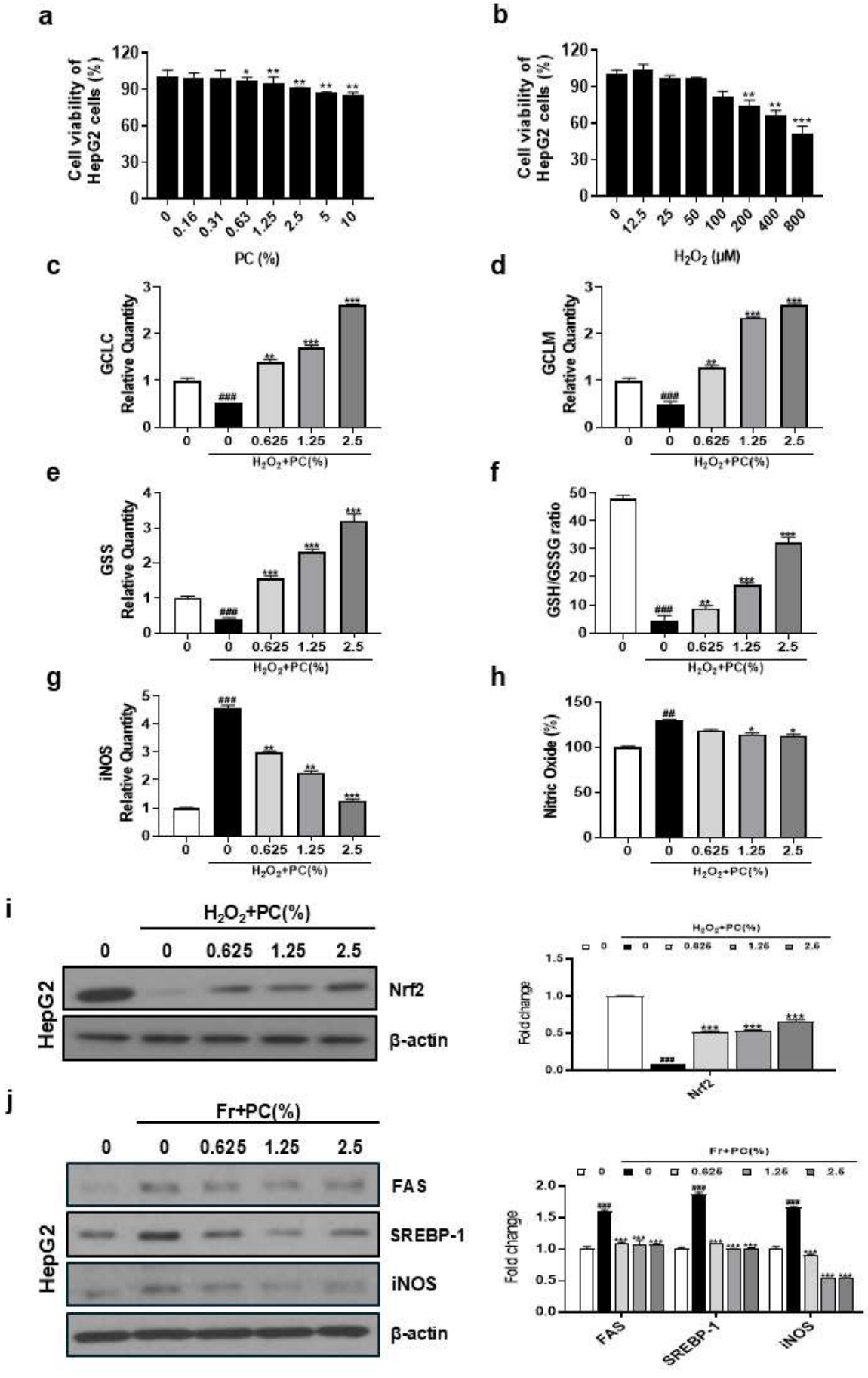

a
Cell viability of HepG2 cells (%)
PC (%)
b
Cell viability of HepG2 cells (%)
H2O2 (μM)
c
GCLC Relative Quantity
H2O2+PC(%)
d
GCLM Relative Quantity
H2O2+PC(%)
e
GSS Relative Quantity
H2O2+PC(%)
f
GSH/GSSG ratio
H2O2+PC(%)
g
iNOS Relative Quantity
H2O2+PC(%)
h
Nitric Oxide (%)
H2O2+PC(%)
i
H2O2+PC(%)
HepG2
Nrf2
β-actin
Fold change
Nrf2
j
Fr+PC(%)
HepG2
FAS
SREBP-1
iNOS
β-actin
Fold change
FAS
SREBP-1
iNOS

Figure 4. Protective effects of PC against H_2O_2-induced oxidative stress and fructose-induced lipogenesis in HepG2 cells. (a) Cell viability of HepG2 cells treated with PC; (b) cell viability of HepG2 cells following H_2O_2 treatment; (c-e) relative mRNA expression levels of GCLC, GCLM, and GSS in 200 μM H_2O_2-stimulated HepG2 cells treated with PC; (f) intracellular GSH/GSSG ratio in HepG2 cells; (g) relative iNOS mRNA expression in H_2O_2-stimulated HepG2 cells; (h) nitric oxide (NO) production in HepG2 cells; (i) Western blot analysis of Nrf2 protein expression in HepG2 cells; (j) Western blot analysis of FAS, SREBP-1, and iNOS protein expression in 10 mM fructose-treated HepG2 cells. Data are presented as the mean ± SD of three independent experiments. The symbol # indicates significant differences compared with the untreated control group, whereas * indicates significant differences compared with the H_2O_2- or fructose-treated group (#/*$p < 0.05$, ##/**$p < 0.01$, ###/***$p < 0.001$).

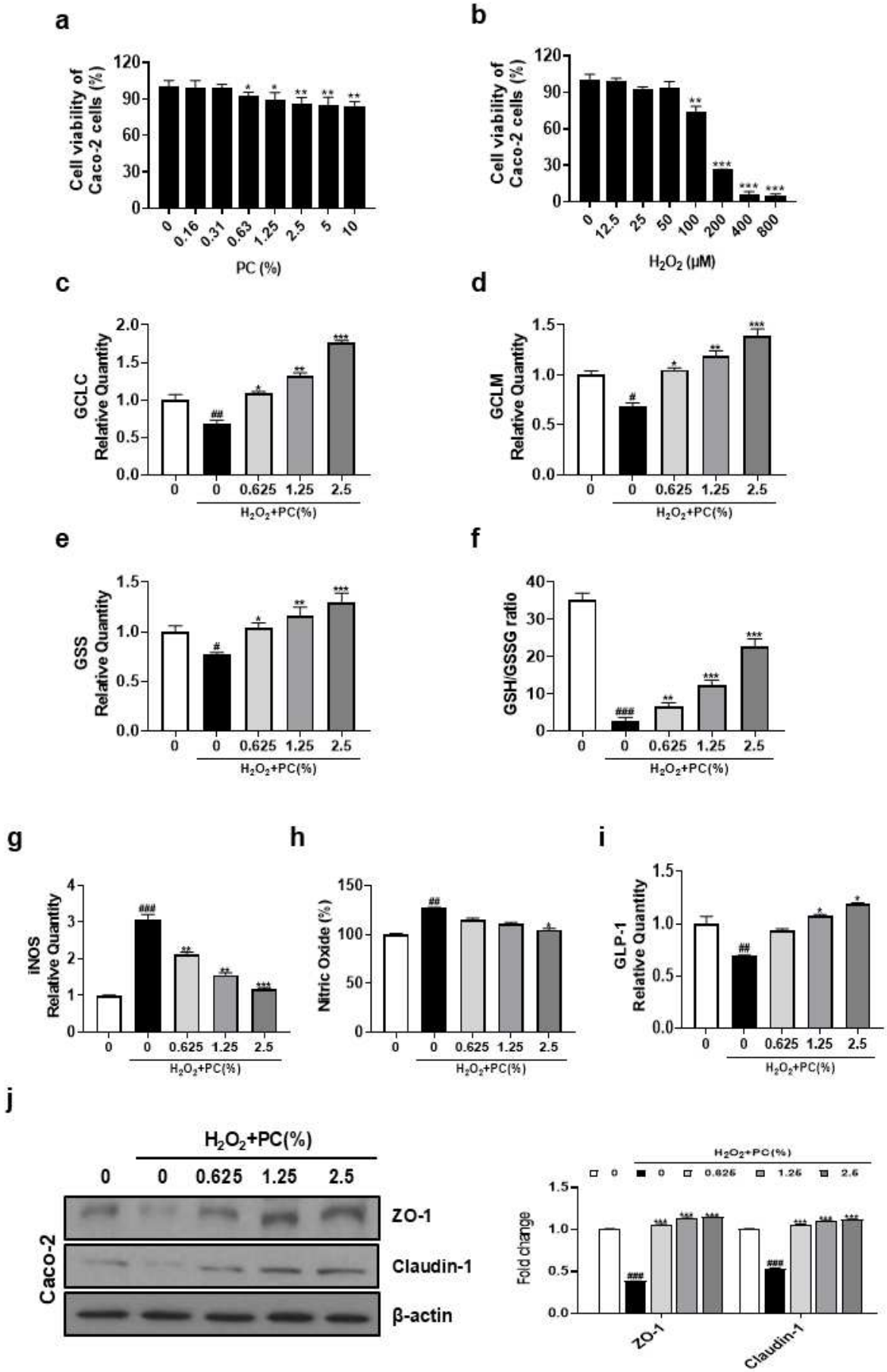

a
Cell viability of Caco-2 cells (%)
PC (%)
b
Cell viability of Caco-2 cells (%)
H2O2 (μM)
c
GCLC Relative Quantity
H2O2+PC(%)
d
GCLM Relative Quantity
H2O2+PC(%)
e
GSS Relative Quantity
H2O2+PC(%)
f
GSH/GSSG ratio
H2O2+PC(%)
g
iNOS Relative Quantity
H2O2+PC(%)
h
Nitric Oxide (%)
H2O2+PC(%)
i
GLP-1 Relative Quantity
H2O2+PC(%)
j
H2O2+PC(%)
Caco-2
ZO-1
Claudin-1
β-actin
Fold change
ZO-1
Claudin-1

Figure 5. Protective effects of PC against H_2O_2-induced oxidative intestinal epithelial injury in Caco-2 cells. (a) Cell viability of Caco-2 cells treated with PC; (b) cell viability of Caco-2 cells following H_2O_2 treatment; (c-e) relative mRNA expression levels of GCLC, GCLM, and GSS in 100 μM H_2O_2-stimulated Caco-2 cells treated with PC; (f) intracellular GSH/GSSG ratio in Caco-2 cells; (g) relative iNOS mRNA expression in H_2O_2-stimulated Caco-2 cells; (h) nitric oxide (NO) production in Caco-2 cells; (i) relative GLP-1 mRNA expression in H_2O_2-stimulated Caco-2 cells; (j) Western blot analysis of ZO-1 and claudin-1 protein expression in Caco-2 cells. Data are presented as the mean ± SD of three independent experiments. The symbol # indicates significant differences compared with the untreated control group, whereas * indicates significant differences compared with the H_2O_2-treated group (#/*$p < 0.05$, ##/**$p < 0.01$, ###/***$p < 0.001$).

4. Discussion

In the present study, we developed a pressed Korean pine leaf juice (PKJ)/coconut water (CW) formulation, designated PC, and evaluated its functional food-applicable properties using chemical antioxidant assays, network-based target prediction, and multiple in vitro cellular models. Previous studies on *P. koraiensis* leaves have primarily focused on extract- or oil-based preparations, including ethanol extracts, essential oils, and supercritical CO_2-extracted oils, which have been associated with antioxidant, anti-inflammatory, anti-cancer, metabolic, antimicrobial, and anti-fatigue activities [1-5]. In contrast, the present study used pressed Korean pine leaf juice (PKJ), a food-compatible aqueous material, thereby providing a processing approach more readily adaptable to beverage-type functional food applications.

A major advantage of using PKJ is the avoidance of organic solvent extraction and the retention of a water-based matrix containing hydrophilic constituents. From a functional food perspective, this approach has practical advantages because it reduces the need for solvent removal, improves compatibility with beverage formulations, and may better reflect consumer-acceptable processing. Green extraction and solvent-reduced processing are increasingly emphasized in natural product and food applications, particularly when safety, sustainability, and food-grade processing are important

considerations [46-51]. Therefore, PKJ may represent a more translationally relevant material than conventional ethanol extracts or volatile oil fractions for developing a daily consumable functional beverage.

The formulation screening showed that PC produced greater DPPH and ABTS radical scavenging activities than PKJ or CW alone and exhibited higher total polyphenol and flavonoid assay values. (Figure 1a and b). ZIP analysis additionally indicated a positive interaction between PKJ and CW (Figure 1c-f). Importantly, the 1:9 formulation retained antioxidant activity comparable to that of the 1:1 formulation despite containing a substantially lower proportion of PKJ, providing an experimental basis for selecting the 1:9 ratio for subsequent evaluation. These findings indicate a formulation-dependent enhancement of antioxidant responses beyond those observed for the individual components. The physicochemical basis underlying this interaction remains to be determined. However, DPPH, ABTS, and Folin-Ciocalteu-based assays are chemical assays that reflect specific redox reactions and do not fully represent biological antioxidant activity, therefore, these findings should be interpreted together with cellular functional assays [48-50,52,53].

Although CW alone showed minimal antioxidant activity and very low total polyphenol and flavonoid contents in this study, coconut water composition is influenced by cultivar, maturity, origin, processing, and storage conditions [8,54-60]. Processed CW may contain lower levels of assay-detectable phenolic compounds than fresh or tender coconut water. Nevertheless, incorporation of CW into the PC formulation was associated with enhanced antioxidant responses and higher total polyphenol and flavonoid assay values compared with the individual components. The physicochemical basis underlying this formulation-dependent effect remains to be determined. The network-based prediction analysis in Figure 2 provided a hypothesis-generating framework for interpreting the subsequent cellular findings. Literature-derived compounds reported from *P. koraiensis* and *C. nucifera* were analyzed, and gallic acid, catechin, and epicatechin were identified as shared candidate phytochemicals. These phenolic compounds are well-known for antioxidant and anti-inflammatory activities and have been reported to modulate inflammatory pathways, oxidative stress responses, and redox-sensitive

signaling [61-65]. Target overlap analysis further identified candidate genes, including BCL2, CASP3, HMOX1, IL6, NFE2L2, and NOS2, which are closely related to apoptosis regulation, antioxidant defense, inflammatory signaling, and nitric oxide production. Importantly, NFE2L2 encodes Nrf2, a master regulator of cellular antioxidant defense, whereas NOS2 encodes iNOS, a key enzyme involved in inflammation-associated nitric oxide production. Thus, the combined TPC/TFC results and literature-based network analysis suggest that phenolic constituents potentially associated with these botanical sources may be related to antioxidant and inflammatory response pathways involving Nrf2/glutathione and iNOS/NO.

Consistent with this prediction, PC suppressed inflammatory responses in LPS-stimulated THP-1 cells. LPS-stimulated THP-1 macrophage-like cells are widely used as an in vitro inflammatory model, in which inflammatory activation induces mediators such as iNOS, NO, TNF-α, and IL-6 [66,67]. In the present study, PC reduced LPS-induced iNOS expression, NO production, and the protein expression of TNF-α and IL-6. These findings indicate that PC has anti-inflammatory activity and that suppression of the iNOS/NO axis may be one of its major functional effects. This result also agrees with the network prediction in Figure 2, in which NOS2 and IL-6 were identified as shared candidate targets.

In HepG2 cells, PC protected against H_2O_2-induced oxidative stress by restoring glutathione-dependent antioxidant defense. H_2O_2 exposure reduced GCLC, GCLM, and GSS expression and decreased the GSH/GSSG ratio, indicating impairment of intracellular redox balance. PC treatment restored these markers and increased Nrf2 protein expression. Because Nrf2 regulates multiple cytoprotective genes involved in antioxidant defense and glutathione metabolism, restoration of Nrf2 expression may contribute to the protective effects of PC against oxidative stress in HepG2 cells [12,68-70]. Previous studies using H_2O_2-treated HepG2 cells similarly reported that antioxidant materials can protect against oxidative stress by reducing ROS/GSSG accumulation, restoring GSH levels, and activating Nrf2-mediated antioxidant responses [14,71,72].

PC also attenuated fructose-induced lipogenic and inflammatory stress in HepG2 cells. Fructose treatment increased FAS and SREBP-1 expression, indicating activation of lipogenic signaling, and

increased iNOS expression, suggesting an accompanying inflammatory stress response [73,74]. PC reduced fructose-induced FAS, SREBP-1, and iNOS expression. These findings suggest that PC may modulate hepatic metabolic stress by suppressing both lipogenesis-related proteins and inflammatory mediators.

The protective effect of PC was further extended to intestinal epithelial cells. In H_2O_2-stimulated Caco-2 cells, PC restored glutathione-related markers, including GCLC, GCLM, and GSS, and recovered the GSH/GSSG ratio. These findings indicate that PC enhances glutathione-dependent antioxidant defense not only in hepatocyte-like cells but also in intestinal epithelial cells. Furthermore, PC suppressed H_2O_2-induced iNOS expression and NO production, indicating that similar antioxidant and inflammatory responses to PC were observed in both HepG2 and Caco-2 cells.

An important additional finding in Caco-2 cells was the restoration of intestinal epithelial functional and barrier-related proteins. H_2O_2-induced oxidative stress is known to disrupt intestinal epithelial barrier function and affect tight junction organization in Caco-2 models. In the present study, H_2O_2 reduced GLP-1 expression and decreased ZO-1 and claudin-1 levels, whereas PC restored these markers. ZO-1 and claudin-1 are important tight junction-associated proteins involved in epithelial barrier integrity, and their restoration suggests that PC may help preserve intestinal epithelial barrier-related responses under oxidative stress conditions. H_2O_2-induced oxidative stress in intestinal epithelial models may impair cellular function and reduce GLP-1 expression, which is relevant to glucose homeostasis [37,75-77].

Taken together, the present findings suggest that PC exerts multi-layered protective effects through interconnected antioxidant, anti-inflammatory, metabolic, and epithelial barrier-related mechanisms. The chemical antioxidant data showed enhanced radical-scavenging responses together with higher total polyphenol and flavonoid assay values in PC. The network analysis predicted candidate targets related to Nrf2-mediated antioxidant defense, iNOS/NO inflammatory signaling, apoptosis regulation, and disease-associated stress pathways. The cellular findings were broadly consistent with these predicted pathways, showing that PC restored glutathione-dependent antioxidant defense, restored Nrf2

expression, suppressed iNOS/NO signaling, and inflammatory cytokine expression, attenuated fructose-induced lipogenic responses, and preserved intestinal barrier-related markers. Taken together, these findings suggest that the effects of PC extend beyond direct chemical radical scavenging and may involve modulation of endogenous cellular redox defense and oxidative inflammatory responses. Rather than focusing on a single molecular pathway, the present study was designed to evaluate the broader functional potential of PC across complementary cellular models. The consistent responses observed in THP-1, HepG2, and Caco-2 cells provide a broader perspective on the antioxidant, anti-inflammatory, metabolic, and intestinal epithelial effects of the formulation. This broad experimental scope, however, did not allow detailed pathway-specific mechanisms to be fully addressed within each individual model. Further studies focusing on selected molecular pathways and in vivo validation will help define the biological basis and functional applicability of PC more comprehensively.

In conclusion, the present study demonstrates that a pressed Korean pine leaf juice-coconut water formulation exhibits enhanced antioxidant-associated responses and attenuates inflammatory, oxidative, metabolic, and intestinal epithelial stress in vitro. The use of PKJ provides a food-compatible and solvent-minimized approach that differs from previously studied ethanol-or oil-based *P. koraiensis* preparations. The experimentally selected 1:9 PKJ formulation restored glutathione-dependent antioxidant defense, reduced inflammatory signaling, attenuated fructose-associated lipogenic responses, and preserved intestinal epithelial barrier-related markers. These findings support further investigation of PC as a functional food formulation.

Author contributions

H.-J.L.; methodology, project administration, supervision, writing-original draft preparation; L.A.; validation, investigation, data curation, software. J.H.; investigation, data curation, and software. All the authors have read and agreed to the published version of the manuscript.

Competing interests

The authors declare no conflict of interest.

Data availability

The datasets generated and/or analyzed during the current study are available from the corresponding author upon reasonable request.

Funding

This research was supported by the National Research Foundation of Korea (NRF) funded by the Ministry of Science and ICT (MSIT), Republic of Korea (Grant No. NRF-2021R1A2C2009095).

Acknowledgements

Not applicable.

References

[1] Cho, S. M., Lee, E. O., Kim, S. H. & Lee, H. J. Essential oil of Pinus koraiensis inhibits cell proliferation and migration via inhibition of p21-activated kinase 1 pathway in HCT116 colorectal cancer cells. BMC Complement. Altern. Med. 14, 275. https://doi.org/10.1186/1472-6882-14-275 (2014).

[2] Valdivieso-Ugarte, M., Gomez-Llorente, C., Plaza-Díaz, J. & Gil, Á. Antimicrobial, antioxidant, and immunomodulatory properties of essential oils: a systematic review. Nutrients 11, 2786. https://doi.org/10.3390/nu11112786 (2019).

[3] Lee, M.-H. et al. Ethanol extract of Pinus koraiensis leaves mitigates high fructose-induced hepatic triglyceride accumulation and hypertriglyceridemia. Appl. Sci. 12, 6745. https://doi.org/10.3390/app12136745 (2022).

[4] Kim, J.-E., Jang, K. T., An, L., Lee, M.-H. & Lee, H.-J. Comparative bioactivities and fatty acid composition of Pinus koraiensis leaf oils obtained using different extraction methods. Life 16, 49. https://doi.org/10.3390/life16010049 (2026).

[5] Lee, S. M. et al. Anti-fatigue potential of Pinus koraiensis leaf extract in an acute exercise-treated mouse model. Biomed. Pharmacother. 153, 113501. https://doi.org/10.1016/j.biopha.2022.113501

(2022).

[6] Platzer, M. et al. Radical scavenging mechanisms of phenolic compounds: a quantitative structure-property relationship (QSPR) study. Front. Nutr. 9, 882458. https://doi.org/10.3389/fnut.2022.882458 (2022).

[7] Yong, J. W., Ge, L., Ng, Y. F. & Tan, S. N. The chemical composition and biological properties of coconut (Cocos nucifera L.) water. Molecules 14, 5144–5164. https://doi.org/10.3390/molecules14125144 (2009).

[8] Shi, S. et al. Research progress in coconut water: a review of nutritional composition, biological activities, and novel processing technologies. Foods 14, 1503. https://doi.org/10.3390/foods14091503 (2025).

[9] Crisman, E. et al. KEAP1-NRF2 protein-protein interaction inhibitors: design, pharmacological properties and therapeutic potential. Med. Res. Rev. 43, 237–287. https://doi.org/10.1002/med.21925 (2023).

[10] Hayes, J. D., Dayalan Naidu, S. & Dinkova-Kostova, A. T. Regulating Nrf2 activity: ubiquitin ligases and signaling molecules in redox homeostasis. Trends Biochem. Sci. 50, 179–205. https://doi.org/10.1016/j.tibs.2024.12.010 (2025).

[11] Dinkova-Kostova, A. T. & Abramov, A. Y. The emerging role of Nrf2 in mitochondrial function. Free Radic. Biol. Med. 88, 179–188. https://doi.org/10.1016/j.freeradbiomed.2015.04.036 (2015).

[12] Harvey, C. J. et al. Nrf2-regulated glutathione recycling independent of biosynthesis is critical for cell survival during oxidative stress. Free Radic. Biol. Med. 46, 443–453. https://doi.org/10.1016/j.freeradbiomed.2008.10.040 (2009).

[13] Chen, X. et al. Glutathione induces Keap1 S-glutathionylation and mitigates oscillating glucose-induced β-cell dysfunction by activating Nrf2. Antioxidants 13, 400. https://doi.org/10.3390/antiox13040400 (2024).

[14] Xu, J. et al. Inhibitory effect of delphinidin on oxidative stress induced by H2O2 in HepG2 cells. Oxid. Med. Cell. Longev. 2020, 4694760. https://doi.org/10.1155/2020/4694760 (2020).

[15] Uchida, Y., Ferdousi, F., Takahashi, S. & Isoda, H. Comprehensive transcriptome profiling of antioxidant activities by glutathione in human HepG2 cells. Molecules 29, 1090. https://doi.org/10.3390/molecules29051090 (2024).

[16] Zhang, M. et al. Reduction of the oxidative damage to H_2O_2-induced HepG2 cells via the Nrf2 signalling pathway by plant flavonoids quercetin and hyperoside. Food Sci. Hum. Wellness 13, 1864–1876. https://doi.org/10.26599/FSHW.2022.9250155 (2024).

[17] Tu, M. et al. 2-Fluorofucose attenuates hydrogen peroxide-induced oxidative stress in HepG2 cells via Nrf2/keap1 and NF-κB signaling pathways. Life 12, 406. https://doi.org/10.3390/life12030406 (2022).

[18] Yu, X. et al. Role of X-box binding protein-1 in fructose-induced de novo lipogenesis in HepG2 cells. Chin. Med. J. 131, 2310–2319. https://doi.org/10.4103/0366-6999.241799 (2018).

[19] Softic, S., Cohen, D. E. & Kahn, C. R. Role of dietary fructose and hepatic de novo lipogenesis in fatty liver disease. Dig. Dis. Sci. 61, 1282–1293. https://doi.org/10.1007/s10620-016-4054-0 (2016).

[20] Geidl-Flueck, B. & Gerber, P. A. Fructose drives de novo lipogenesis affecting metabolic health. J. Endocrinol. 257, e220270. https://doi.org/10.1530/JOE-22-0270 (2023).

[21] Howes, M. T., King, J. & Rosengren, R. J. Effects of fructose on features of steatotic liver disease in HepG2 cells. Nutrients 17, 2762. https://doi.org/10.3390/nu17172762 (2025).

[22] Ferré, P. & Foufelle, F. Hepatic steatosis: a role for de novo lipogenesis and the transcription factor SREBP-1c. Diabetes Obes. Metab. 12 (Suppl. 2), 83–92. https://doi.org/10.1111/j.1463-1326.2010.01275.x (2010).

[23] Chanput, W., Mes, J., Vreeburg, R. A., Savelkoul, H. F. & Wichers, H. J. Transcription profiles of LPS-stimulated THP-1 monocytes and macrophages: a tool to study inflammation modulating effects

582 of food-derived compounds. Food Funct. 1, 254–261. https://doi.org/10.1039/c0fo00113a (2010).

583 [24] Shu, J. et al. Human amnion mesenchymal cells inhibit lipopolysaccharide-induced TNF-α and IL-
584 1β production in THP-1 cells. Biol. Res. 48, 69. https://doi.org/10.1186/s40659-015-0062-3 (2015).

585 [25] Tedesco, S. et al. Convenience versus biological significance: are PMA-differentiated THP-1 cells
586 a reliable substitute for blood-derived macrophages when studying in vitro polarization? Front.
587 Pharmacol. 9, 71. https://doi.org/10.3389/fphar.2018.00071 (2018).

588 [26] Yoon, Y. K., Woo, H. J. & Kim, Y. Orostachys japonicus inhibits expression of the TLR4, NOD2,
589 iNOS, and COX-2 genes in LPS-stimulated human PMA-differentiated THP-1 cells by inhibiting NF-
590 κB and MAPK activation. Evid.-Based Complement. Altern. Med. 2015, 682019.
591 https://doi.org/10.1155/2015/682019 (2015).

592 [27] Sharif, O., Bolshakov, V. N., Raines, S., Newham, P. & Perkins, N. D. Transcriptional profiling of
593 the LPS induced NF-kappaB response in macrophages. BMC Immunol. 8, 1.
594 https://doi.org/10.1186/1471-2172-8-1 (2007).

595 [28] Chelakkot, C., Ghim, J. & Ryu, S. H. Mechanisms regulating intestinal barrier integrity and its
596 pathological implications. Exp. Mol. Med. 50, 1–9. https://doi.org/10.1038/s12276-018-0126-x (2018).

597 [29] Arumugam, P., Saha, K. & Nighot, P. Intestinal epithelial tight junction barrier regulation by novel
598 pathways. Inflamm. Bowel Dis. 31, 259–271. https://doi.org/10.1093/ibd/izae232 (2025).

599 [30] Lee, S. H. Intestinal permeability regulation by tight junction: implication on inflammatory bowel
600 diseases. Intest. Res. 13, 11–18. https://doi.org/10.5217/ir.2015.13.1.11 (2015).

601 [31] Zhang, Z. et al. PEAK1 maintains tight junctions in intestinal epithelial cells and resists colitis by
602 inhibiting autophagy-mediated ZO-1 degradation. Nat. Commun. 16, 6777.
603 https://doi.org/10.1038/s41467-025-62107-z (2025).

604 [32] Rodgers, L. S., Beam, M. T., Anderson, J. M. & Fanning, A. S. Epithelial barrier assembly requires
605 coordinated activity of multiple domains of the tight junction protein ZO-1. J. Cell Sci. 126, 1565–1575.

https://doi.org/10.1242/jcs.113399 (2013).

[33] Suzuki, T. Regulation of intestinal epithelial permeability by tight junctions. Cell. Mol. Life Sci. 70, 631–659. https://doi.org/10.1007/s00018-012-1070-x (2013).

[34] Rao, R. K., Baker, R. D., Baker, S. S., Gupta, A. & Holycross, M. Oxidant-induced disruption of intestinal epithelial barrier function: role of protein tyrosine phosphorylation. Am. J. Physiol. 273, G812–G823. https://doi.org/10.1152/ajpgi.1997.273.4.G812 (1997).

[35] Chuenkitiyanon, S., Pengsuparp, T. & Jianmongkol, S. Protective effect of quercetin on hydrogen peroxide-induced tight junction disruption. Int. J. Toxicol. 29, 418–424. https://doi.org/10.1177/1091581810366487 (2010).

[36] Wang, N. et al. Resveratrol protects oxidative stress-induced intestinal epithelial barrier dysfunction by upregulating heme oxygenase-1 expression. Dig. Dis. Sci. 61, 2522–2534. https://doi.org/10.1007/s10620-016-4184-4 (2016).

[37] Huang, T. T., Gu, P. P., Zheng, T., Gou, L. S. & Liu, Y. W. Piperine, as a TAS2R14 agonist, stimulates the secretion of glucagon-like peptide-1 in the human enteroendocrine cell line Caco-2. Food Funct. 13, 242–254. https://doi.org/10.1039/d1fo02932k (2022).

[38] Caron, J., Domenger, D., Dhulster, P., Ravallec, R. & Cudennec, B. Using Caco-2 cells as novel identification tool for food-derived DPP-IV inhibitors. Food Res. Int. 92, 113–118. https://doi.org/10.1016/j.foodres.2017.01.002 (2017).

[39] Nadkarni, P., Chepurny, O. G. & Holz, G. G. Regulation of glucose homeostasis by GLP-1. Prog. Mol. Biol. Transl. Sci. 121, 23–65. https://doi.org/10.1016/B978-0-12-800101-1.00002-8 (2014).

[40] Singleton, V. L. & Rossi, J. A. Colorimetry of total phenolics with phosphomolybdic-phosphotungstic acid reagents. Am. J. Enol. Vitic. 16, 144–158 (1965).

[41] Davis, W. B. Determination of flavanones in citrus fruits. Anal. Chem. 19, 476–478. https://doi.org/10.1021/ac60007a016 (1947).

[42] Blois, M. S. Antioxidant determinations by the use of a stable free radical. Nature 181, 1199–1200. https://doi.org/10.1038/1811199a0 (1958).

[43] Verzelloni, E., Tagliazucchi, D. & Conte, A. Relationship between the antioxidant properties and the phenolic and flavonoid content in traditional balsamic vinegar. Food Chem. 105, 564–571. https://doi.org/10.1016/j.foodchem.2007.04.014 (2007).

[44] Han, H., Kim, J.-E. & Lee, H.-J. Effect of apigetrin in pseudo-SARS-CoV-2-induced inflammatory and pulmonary fibrosis in vitro model. Sci. Rep. 14, 14545. https://doi.org/10.1038/s41598-024-65447-w (2024).

[45] Green, L. C. et al. Analysis of nitrate, nitrite, and [15N]nitrate in biological fluids. Anal. Biochem. 126, 131–138. https://doi.org/10.1016/0003-2697(82)90118-X (1982).

[46] Chemat, F., Vian, M. A. & Cravotto, G. Green extraction of natural products: concept and principles. Int. J. Mol. Sci. 13, 8615–8627. https://doi.org/10.3390/ijms13078615 (2012).

[47] Chemat, F. et al. Review of alternative solvents for green extraction of food and natural products: panorama, principles, applications and prospects. Molecules 24, 3007. https://doi.org/10.3390/molecules24163007 (2019).

[48] Mirzazadeh, N. et al. Comparison of different green extraction methods used for the extraction of anthocyanin from red onion skin. Food Sci. Nutr. 12, 7347–7357. https://doi.org/10.1002/fsn3.4354 (2024).

[49] Câmara, J. S. et al. Green extraction techniques as advanced sample preparation approaches in biological, food, and environmental matrices: a review. Molecules 27, 2953. https://doi.org/10.3390/molecules27092953 (2022).

[50] Cannavacciuolo, C., Pagliari, S., Celano, R., Campone, L. & Rastrelli, L. Critical analysis of green extraction techniques used for botanicals: trends, priorities, and optimization strategies—a review. TrAC Trends Anal. Chem. 173, 117627. https://doi.org/10.1016/j.trac.2024.117627 (2024).

[51] Putra, N. R. et al. Advancements and challenges in green extraction techniques for Indonesian natural products: a review. S. Afr. J. Chem. Eng. 46, 88–98. https://doi.org/10.1016/j.sajce.2023.08.002 (2023).

[52] Wołosiak, R. et al. Verification of the conditions for determination of antioxidant activity by ABTS and DPPH assays—a practical approach. Molecules 27, 50. https://doi.org/10.3390/molecules27010050 (2022).

[53] Pérez, M., Dominguez-López, I. & Lamuela-Raventós, R. M. The chemistry behind the Folin-Ciocalteu method for the estimation of (poly)phenol content in food: total phenolic intake in a Mediterranean dietary pattern. J. Agric. Food Chem. 71, 17543–17553. https://doi.org/10.1021/acs.jafc.3c04022 (2023).

[54] Prades, A., Dornier, M., Diop, N. & Pain, J.-P. Coconut water uses, composition and properties: a review. Fruits 67, 87–107. https://doi.org/10.1051/fruits/2012002 (2012).

[55] Jackson, J. C., Gordon, A., Wizzard, G., McCook, K. & Rolle, R. Changes in chemical composition of coconut (Cocos nucifera) water during maturation of the fruit. J. Sci. Food Agric. 84, 1049–1052. https://doi.org/10.1002/jsfa.1783 (2004).

[56] Cunha, A. G. et al. Chemical composition of thermally processed coconut water evaluated by GC-MS, UPLC-HRMS, and NMR. Food Chem. 324, 126874. https://doi.org/10.1016/j.foodchem.2020.126874 (2020).

[57] Detudom, R. et al. Dynamic changes in physicochemical and microbiological qualities of coconut water during postharvest storage under different conditions. Horticulturae 9, 1284. https://doi.org/10.3390/horticulturae9121284 (2023).

[58] Shayanthavi, S., Kapilan, R. & Wickramasinghe, I. Comprehensive analysis of physicochemical, nutritional, and antioxidant properties of various forms and varieties of tender coconut (Cocos nucifera L.) water in Northern Sri Lanka. Food Chem. Adv. 4, 100645. https://doi.org/10.1016/j.focha.2024.100645 (2024).

679 [59] Hou, M. et al. Dynamics of flavonoid metabolites in coconut water based on metabolomics
680 perspective. Front. Plant Sci. 15, 1468858. https://doi.org/10.3389/fpls.2024.1468858 (2024).

681 [60] Jiang, R. et al. Comparative study of the fatty acid and phenolic profiles of tender and mature
682 coconut for coconut milk production. Foods 14, 4023. https://doi.org/10.3390/foods14234023 (2025).

683 [61] Yang, D.-J. et al. Anti-inflammatory activity of epicatechin. J. Food Biochem. 39, 334–343.
684 https://doi.org/10.1111/jfbc.12134 (2015).

685 [62] Yilmaz, Y. & Toledo, R. T. Major flavonoids in grape seeds and skins: antioxidant capacity of
686 catechin, epicatechin, and gallic acid. J. Agric. Food Chem. 52, 255–260.
687 https://doi.org/10.1021/jf030117h (2004).

688 [63] Oriakhi, K. & Orumwensodia, K. O. Combinatorial effect of gallic acid and catechin on some
689 biochemical and pro-inflammatory markers in CCl_4-mediated hepatic damage in rats. Phytomed. Plus
690 1, 100017. https://doi.org/10.1016/j.phyplu.2020.100017 (2021).

691 [64] Liu, W. et al. Phenolic metabolites as therapeutic in inflammation and neoplasms: molecular
692 pathways explaining their efficacy. Pharmacol. Res. 193, 106812.
693 https://doi.org/10.1016/j.phrs.2023.106812 (2023).

694 [65] Kim, J. M. & Heo, H. J. The roles of catechins in regulation of systemic inflammation. Food Sci.
695 Biotechnol. 31, 957–970. https://doi.org/10.1007/s10068-022-01069-0 (2022).

696 [66] Ozleyen, A., Yilmaz, Y. B. & Tumer, T. B. Dataset on the differentiation of THP-1 monocytes to
697 LPS inducible adherent macrophages and their capacity for NO/iNOS signaling. Data Brief 35, 106786.
698 https://doi.org/10.1016/j.dib.2021.106786 (2021).

699 [67] Fukuda, K. et al. Inhibition by parthenolide of phorbol ester-induced transcriptional activation of
700 inducible nitric oxide synthase gene in a human monocyte cell line THP-1. Biochem. Pharmacol. 60,
701 595–600. https://doi.org/10.1016/S0006-2952(00)00340-3 (2000).

702 [68] Iranshahy, M., Iranshahi, M., Abtahi, S. R. & Karimi, G. The role of nuclear factor erythroid 2-

related factor 2 in hepatoprotective activity of natural products: a review. Food Chem. Toxicol. 120, 261–276. https://doi.org/10.1016/j.fct.2018.07.024 (2018).

[69] Zhou, J., Zheng, Q. & Chen, Z. The Nrf2 pathway in liver diseases. Front. Cell Dev. Biol. 10, 826204. https://doi.org/10.3389/fcell.2022.826204 (2022).

[70] Galicia-Moreno, M. et al. Roles of Nrf2 in liver diseases: molecular, pharmacological, and epigenetic aspects. Antioxidants 9, 980. https://doi.org/10.3390/antiox9100980 (2020).

[71] Mani, M. et al. Activation of Nrf2-antioxidant response element mediated glutamate cysteine ligase expression in hepatoma cell line by homocysteine. Hepat. Mon. 13, e8394. https://doi.org/10.5812/hepatmon.8394 (2013).

[72] Chiangsom, A. et al. Protective effect of Phikud Navakot extract against hydrogen peroxide-induced oxidative stress in HepG2 cells. Thai J. Pharm. Sci. 43(4), 186–194. https://doi.org/10.56808/3027-7922.3052 (2019).

[73] Zhao, L. et al. Fructose and glucose combined with free fatty acids induce metabolic disorders in HepG2 cell: a new model to study the impacts of high-fructose/sucrose and high-fat diets in vitro. Mol. Nutr. Food Res. 60, 909–921. https://doi.org/10.1002/mnfr.201500635 (2016).

[74] Todoric, J. et al. Fructose stimulated de novo lipogenesis is promoted by inflammation. Nat. Metab. 2, 1034–1045. https://doi.org/10.1038/s42255-020-0261-2 (2020).

[75] Herring, T. A., Cuppett, S. L. & Zempleni, J. Genomic implications of H(2)O(2) for cell proliferation and growth of Caco-2 cells. Dig. Dis. Sci. 52, 3005–3015. https://doi.org/10.1007/s10620-006-9663-6 (2007).

[76] Urbauer, E. et al. Reduced intestinal GLP-1+ cell numbers are associated with an inflammation-related epithelial metabolic signature. Cell. Mol. Gastroenterol. Hepatol. 20, 101656. https://doi.org/10.1016/j.jcmgh.2025.101656 (2026).

[77] Rowlands, J., Heng, J., Newsholme, P. & Carlessi, R. Pleiotropic effects of GLP-1 and analogs on

727 cell signaling, metabolism, and function. Front. Endocrinol. 9, 672.
728 https://doi.org/10.3389/fendo.2018.00672 (2018).

Supplementary Files

This is a list of supplementary files associated with this preprint. Click to download.

- SupplementaryInformation.pdf